Paper presented at the 1st International Conf. on Motion and Vibration Control, Yokohama, September 1992
Session : Information Instruments

VIBRATION AND DEFLECTION OF A SILICON-WAFER SLICER CUTTING THE CRYSTAL INGOT

Seiji Chonan and Zhong-wei Jiang
Department of Engineering Science, Tohoku University, Aramakiaza Aoba, Aoba-ku, Sendai, 980 Japan
Yasuhiro Yuki
Toyo Engineering, Co., Ltd., Japan

ABSTRACT

Vibration and deflecton of a silicon-wafer slicer cutting the crystal ingot is studied analytically. The blade is clamped at the outer boundary and stressed initially in the radial direction, while the inner periphery is subjected to distributed in-plane and lateral slicing loads from the workpiece. The stresses from the tensioning, spinning and loading from the workpiece are taken into account in the stress distribution in the blade. The solution is obtained by introducing the multi-modal expansion and applying the Galerkin method to the governing equation of the blade. Numerical results are presented for an actual SUS 301 blade cutting a 6″ diameter silicon ingot. Results obtained show that the initial tensioning has a significant effect on the natural frequencies of the blade, while the lateral deflection of the blade is much affected by the lateral reaction force from the ingot.

KEY WORDS: vibration, deflecton, silicon-wafer slicer, crystal ingot.

INTRODUCTION

Information-intensive culture has accelerated the development and production of computers and their peripheral equipments, which also has stimulated the development of semiconductor industry and accelerated the production of silicon wafers.

The ID(inner-diameter) saw blade is nowadays commonly used in the crystal wafering. It is a thin annular blade with diamond abrasive at the inner edge while clamped along the the outer periphery. The blade is tensioned initially at the outer edge to increase the stiffness. Still, the blade vibration and the lateral displacement can cause the degradation of the blade flatness and leads to a damage of the wafers. It is therefore of technological importance to investigate the behaviours of the ID saw blade cutting the crystal ingot.

A lot of papers have been published on the vibration characteristics of spinning blades. Most of them are concerned with the blade that is clamped at the center and free along the outer edge. Iwan and Moeller[1] studied the stability of a spinning clamped-free elastic disk moving in contact with a stationary mass, spring, and dashpot. Radcliffe and Mote[2] and Srinivasan and Ramamurti[3]) extended the buckling and vibration stability theories for centrally clamped rotating disks to include the effects of concentrated inclined edge loads. Benson and Bogy[4] addressed the problem of steady deflection of a very flexible spinning disk to transverse loads that are fixed in space. Further, Ferguson and White[5] studied the free vibration characteristics of a clamped-free disk under the action of a static in-plane peripheral load and having the constraint at the outer periphery. Jiang et al.[6][7] studied the steady state response of a read/write head floppy disk system to axial and pitching oscillations. As for the free-clamped blade, only a few papers have been published during the past years. Forman and Rhines[8] obtained the natural frequencies and associated mode shapes of the crystal slicing ID saw blade. The effect of stresses from initial tensioning was taken into acount, while the flexural rigidity of blade and the stresses from rotation were ignored. Chonan and Sato[9] investigated the flexural vibration and stability of freely rotating free-clamped blades. Further, Chonan et al.[10] obtained the in-plane stress distribution in a silicon-wafer slicer cutting the crystal ingot.

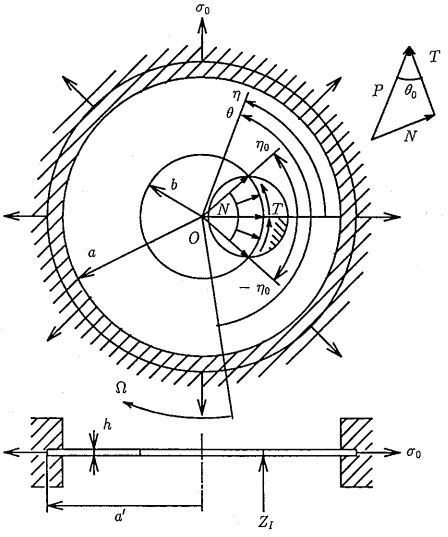

Fig. 1. Geometry of problem and co-ordinates.

This paper is a study on the vibration and deflection of a silicon-wafer slicer cutting the cylindrical crystal ingot. The stresses in the blade caused from the tensioning, spinning and loading from the workpiece are all taken into account in the analysis. The solution is obtained by introducing the method of multi-modal expansion and applying the Galerkin method to the governing equations of the system. Numerical results are presented for an actual SUS 301 blade cutting a 6″diameter silicon ingot at 1550rpm.

FORMULATION AND ANALYSIS

Figure 1 shows an ID saw blade slicing a silicon ingot at a constant angular speed Ω. The blade has a thickness h and is free at an inner radius ($r = b$). After tensioned in the radial direction at the outer radius ($r = a'$), the blade is clamped from both sides by rigid rings in the range $r = a - a'$. In the figure, the (r,θ) is the co-ordinate frame rotating with the blade, while the (r,η) the frame fixed in space. The inner periphery of the blade is acted upon by the radial compressive force N (N/m^2) and the circumferential shear force T (N/m^2), both of which are distributed uniformly over the arc $| \eta | \leq \eta_0$. The resultant of N and T is denoted by P, and the inclination of P to T by θ_0 as shown in the figure. In the analysis that follows, the lateral (out-of-plane) force acting uniformly along the inner periphery $| \eta | \leq \eta_0$ is approximated by a series of concentrated lateral forces. By denoting the concentrated force at the point (r_k,η_k) by q_k, the lateral force $q(r,\eta,t)$ acting on the plate is written as

$$q(r,\eta,t) = \sum_{k=1}^{K} q_k(1/r)\delta(r - r_k)\delta(\eta - \eta_k), \qquad \sum_{k=1}^{K} q_k = Z_I, \tag{1}$$

where $\delta(\ )$ is the Dirac delta function, Z_I is the resultant lateral force acting on the plate, and K is the total number of concentrated forces assumed.

The stresses in the blade cutting the silicon ingot are, with respect to the co-ordinate frame fixed in space (r,η), (Chonan et al., 1991)

$$\sigma_r(r,\eta) = \sigma_{Cr}(r) + \sigma_{Br}(r) + \sigma_{Nr}(r,\eta) + \sigma_{Tr}(r,\eta), \tag{2}$$
$$\sigma_\theta(r,\eta) = \sigma_{C\eta}(r) + \sigma_{B\eta}(r) + \sigma_{N\eta}(r,\eta) + \sigma_{T\eta}(r,\eta), \tag{3}$$
$$\tau_{r\eta}(r,\eta) = \tau_{Nr\eta}(r,\eta) + \tau_{Tr\eta}(r,\eta). \tag{4}$$

Here, σ_r is the in-plane, radial normal stress, σ_η the hoop stress, and $\tau_{r\eta}$ the shear stress in the blade; $\sigma_{Cr}(r)$ and $\sigma_{C\eta}(r)$ are the stresses due to the initial tension σ_0 along the outer periphery $r = a'$, and $\sigma_{Br}(r)$ and $\sigma_{B\eta}(r)$ are the stresses induced by the centrifugal force from the blade rotation; non-axisymmetric stresses represented by $\sigma_{N\eta r}(r,\eta) - \tau_{Tr\eta}(r,\eta)$ are the stresses due to the in-plane reaction force from the sliced ingot at the inner periphery.

The governing equation for the flexural vibration of the blade referred to the co-ordinate frame fixed in space is

$$\begin{aligned} &D[\partial^2/\partial r^2 + (1/r)\partial/\partial r + (1/r)^2\partial^2/\partial\eta^2]^2 w + \rho h[\partial/\partial t - \Omega\partial/\partial\eta]^2 w \\ &- h[(1/r)\partial/\partial r(r\sigma_r \partial w/\partial r) + (1/r^2)\partial/\partial\eta(\sigma_\eta \partial w/\partial\eta) + (1/r)\partial/\partial r(\tau_{r\eta}\partial w/\partial\eta) + (1/r)\partial/\partial\eta(\tau_{r\eta}\partial w/\partial r)] \\ &= \sum_{k=1}^{K} q_k(1/r)\delta(r - r_k)\delta(\eta - \eta_k), \end{aligned} \tag{5}$$

where $w(r,\eta,t)$ is the lateral displacement of the blade, $D(= Eh^3/12(1-\nu^2))$ is the flexural rigidity, E is the young's modulus, ν is the Poisson ratio and ρ is the mass density of the blade.

One assumes the solution of equation (5) in a series form

$$w(r,\eta,t) = \sum_{m=0}^{M}\sum_{n=0}^{N}[C_{mn}(t)\cos(n\eta) + S_{mn}(t)\sin(n\eta)]R_{mn}(r). \tag{6}$$

Here, R_{mn} is the mode function of a non-rotating stationary blade with a free inner edge ($r = b$) while clamped along the outer boudary ($r = a$), and m and n are the numbers of modal circles and diameters on the blade. R_{mn} is given by

$$R_{mn}(r) = J_n(k_{mn}r) + F_{mn}Y_n(k_{mn}r) + G_{mn}I_n(k_{mn}r) + H_{mn}K_n(k_{mn}r), \tag{7}$$

where J_n and Y_n are Bessel functions of the first and second kinds, and I_n and K_n are modified Bessel functions ; $F_{mn} - H_{mn}$ are unknowns and k_{mn}'s are eigenvalues determined from the boundary conditions of the blade.

Substituting equation (6) into equation (5), further applying Galerkin method to the resulting equation, one has a system of simultaneous ordinary differential equations of the form

$$M\ddot{X} + \Gamma\dot{X} + KX = Q, \tag{8}$$

where

$$X = [C_{00}(t), C_{01}(t), S_{01}(t), \cdots, C_{mn}(t), S_{mn}(t)]^{\mathrm{T}}.$$

Here, M, Γ, and K are the matrices of the dimension $[(p+1)(2q+1)] \times [(p+1)(2q+1)]$, and Q the column vector which is appeared due to the lateral loading at the disk inner periphery.

Equation (8) reduces to that of the natural vibration when one puts $Q = 0$. In this case, the equation is further modified as

$$\dot{a} = Ha, \tag{9}$$

where

$$a = [X,\ \dot{X}]^{\mathrm{T}},\quad H = \begin{bmatrix} 0 & I \\ -M^{-1}K & -M^{-1}\Gamma \end{bmatrix}.$$

Substituting

$$a = A\exp(i\omega t) \tag{10}$$

into equation (9), one has

$$|H - i\omega I| = 0. \tag{11}$$

This is the frequency equation for a freely rotating blade with the in-plane slicing load at the inner periphery. On the other hand, when one assumes that a long time has passed since the lateral force was applied to the blade, one obtains the steady state response of the blade from

$$KX = Q. \tag{12}$$

After having X from the above equation, the displacement of the blade is determined from

$$w(r,\eta) = \sum_{m=0}^{M}\sum_{n=0}^{N}[C_{mn}\cos(n\eta) + S_{mn}\sin(n\eta)]R_{mn}(r). \tag{13}$$

Table 1. Physical Parameters of Slicing Blade

$a' = 0.3125$ (m)	$\nu = 0.28$
$a = 0.298$ (m)	$\rho = 7.84 \times 10^3$(kg/m^3)
$b = 0.120$ (m)	$E = 1.99 \times 10^{11}$ (N/m^2)
$h = 0.15 \times 10^{-3}$ (m)	$\sigma_0 = 7.05 \times 10^8$ (N/m^2)

Table 2. Edge Loading Distribution

η_0	$P(\times 10^4$N/m$^2)$	θ_0	Z_I (N)
10°	154.08	66.79°	0.49
20°	277.10	75.09°	2.06
30°	290.74	74.89°	3.14
39.42°	295.50	74.10°	4.32

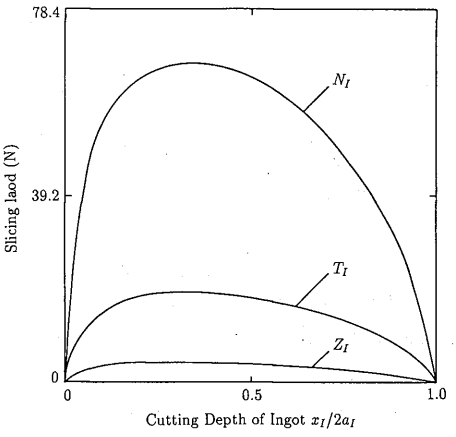

Fig. 2. Slicing load (measured).

NUMERICAL RESULTS AND DISCUSSIONS

Numerical results that follow are for a SUS 301 blade of inner radius 0.120 m, outer radius 0.3125 m and thickness 0.15 mm cutting the slicon ingot. The physical parameters measured are shown in Table 1. σ_0 is the initial tension applied at the outer periphery ($r = a'$) for which the inner hole of the blade is widened by $\Delta b = 1$mm.

The depth of cut of the ingot, x_I, is a function of the angle of contact η_0 between the ingot and the slicing blade, i.e.,

$$x_I(\eta_0) = \begin{cases} a_I - b(1-\cos\eta_0) - (a_I^2 - b^2\sin^2\eta_0)^{1/2} & \text{for } 0 \le x_I(\eta_0) \le x_I(\eta_{0MAX}), \\ a_I - b(1-\cos\eta_0) + (a_I^2 - b^2\sin^2\eta_0)^{1/2} & \text{for } x_I(\eta_{0MAX}) < x_I(\eta_0) \le 2a_I. \end{cases} \tag{14}$$

Here, a_I is the radius of ingot, and $\eta_{0max}(=\arcsin(a_I/b))$ is the maximum contacting angle between the blade and the ingot.

Figure 2 shows the variation of the slicing load measured for an actual sawblade cutting a 6″ diameter silicon ingot. In the figure, N_I and T_I are respectively the resultant in-plane radial and circumferential cutting forces, while Z_I is the lateral force acting on the inner edge from the ingot. Combining Figure 2 with equation (14), one can describe the variation of the loads as functions of the contacting angle η_0. Some results are presented in Table 2. The slicing loads at $\eta_0 = 30°$ correspond to the loads at the depth of cut $x_I = 13.15$ mm in Figure 2.

Figures 3(a)–(c) show the variations of the radial normal and circumferential hoop stresses, σ_r and σ_η, and the shear stress $\tau_{r\eta}$ along the $\eta = 0°$ line for the case of load distribution $\eta_0 = 30°$. In the figures, the curve

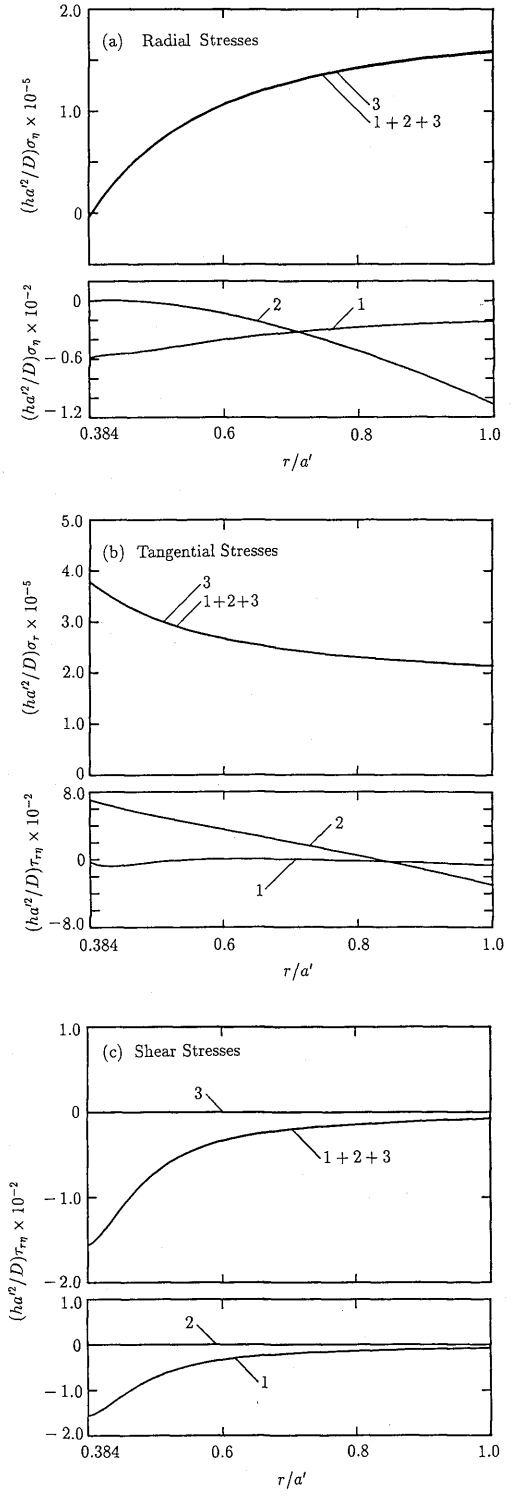

Fig. 3. In-plane stresses versus radial coordinate;
Curve1=Stress from slicing edge load; Curve2 =Stress from rotation; Curve3=Stress from tensioning at the outer edge; $\eta = 0°$, $\Omega = 1550$ rpm, $P = 290.74 \times 10^4$ N/m^2, $\theta_0 = 74.89°$, $\eta_0 = 30.00°$, $\sigma_0 = 7.05 \times 10^8$ N/m^2. (a) Radial Stresses; (b) Tangential Stresses; (c) Shear Stresses.

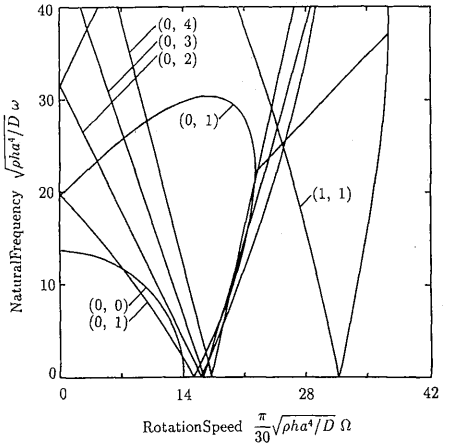

Fig. 4. Natural frequencies of laterally vibrating blade versus the rotation speed; $P = 0$ N/m^2, $\sigma_0 = 0$ N/m^2.

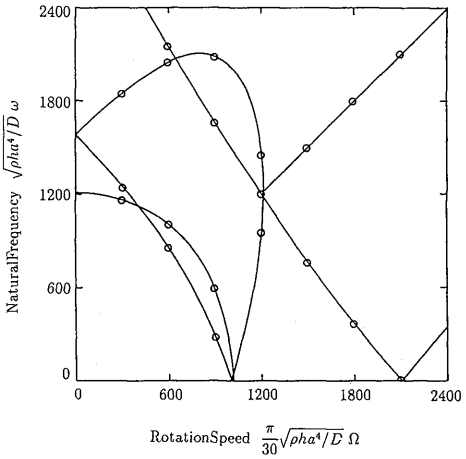

Fig. 5. Effect of the slicing load on natural frequncies; ($\sigma_0 = 7.05 \times 10^8$ N/m^2)
— Natural frequencies without slicing load ($P = 0$ N/m^2);
o Natural frequencies with slicing load ($P = 290.74 \times 10^4$ N/m^2, $\theta_0 = 74.89°$, $\eta_0 = 30°$).

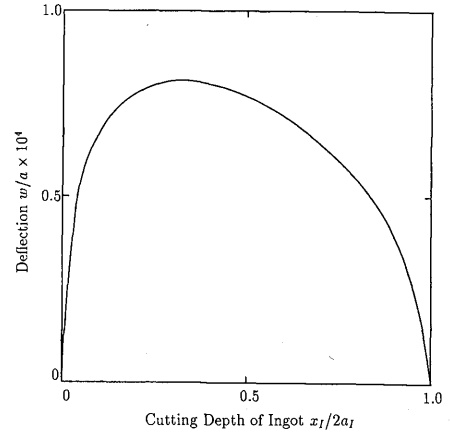

Fig. 6. Deflection of the blade inner edge versus cutting depth of ingot; $a_I = 0.1524$ m, $\eta = 0°$, $\Omega = 1550$ rpm, $\sigma_0 = 7.05 \times 10^8$ N/m^2.

1 is the stress from the sliced ingot, the curve 2 the stress induced by the centrifugal force at the rotation 1550 rpm, and the curve 3 the stress from the initial tensioning along the blade outer periphery $r = a'$. The curve 1+2+3 is the actual, resultant stress given by the superposition of curves 1 through 3. For the cases of normal and hoop stress distributions (Figures 3(a) and (b)), the streses from the slicing load and the centrifugal force are negligibly small compared with the stress from the tensioning at the outer edge. The shear stress (Figure 3(c)) is just the stress from the slicing load, since the centrifugal force and the initial radial tension are both axisymmetric and induce no shear stresses in the blade. The results that follow are for the blade with the stress distribution presented in Figures 3(a)–(c).

Figures 4 and 5 show the variations of natural frequencies of laterally vibrating blade versus the rotation speed. Figure 4 is the result for the blade with no slicing load ($P = 0$ N/m^2), and no initial tensioning ($\sigma_0 =$ 0 N/m^2). The symbol (m,n) indicates that the curve is for the frequency of the mode with m nodal circles and n nodal diameters on the blade. It is seen that each mode, except the (0,0) mode, has two natural frequencies for a speed of revolution. The higher frequency is the one for the flexural wave travelling in the same direction as the blade rotation, while the lower frequency is the frequency for the regressive wave propagating in the opposite direction to the blade rotation. It is seen that the frequency of the backward wave deceases monotonously with an increase of the rotation speed. After decreasing to zero, it again increases when the rotation speed increases further. The frequency of the forwarding wave, on the other hand, first becomes greater with an increase of the rotation speed. However, after ariving at the maximum it then decreases and coalesces with the frequency of the backward wave. After the coalescence, the two frequencies take complex conjugate values. A flutter type of instability appears on the blade if the rotation speed increases further. The frequency of fundamental (0,0) mode decreases as the rotation speed increases. After arriving at zero it then takes a purely imaginery value if the speed becomes higher. The rotation speed at which the frequency drops to zero is the speed that brings about a divergence type of instability on the blade. The blade in this case is buckled by the centrifugal force from the rotation.

Figure 5 shows the frequencies of the blade having an initial tension $\sigma_0 = 7.05\times10^8$ N/m^2. The solid lines are the frequencies for the blade with no slicing load ($P = 0$ N/m^2), while the circles in the figure show the frequencies for the blade whth a slicing load ($P = 290.74\times10^4$ N/m^2, $\theta_0 = 74.89°$, $\eta_0 = 30°$) at the inner edge. It is found that the slicing load has no considerable effect on the blade frequencies. Further, comparison with Figure 4 shows that the natural frequencies are increased significantly by the initial tensioning of the blade. For the operation speed of 1550 rpm or for the nondimensional rotation speed $(\pi/30)\sqrt{\rho h a^4/D}\Omega =$ 63.43, the blade without initial tension is unstable due to the buckling. It is said that the stress from the initial tensioning increases the blade stiffness and stabilizes the blade response.

Next, one obtains the deflection of the blade that is cutting a 6″ diameter silicon ingot. In the calculation, the lateral load was approximated by concentrated forces uniformly distributed over 100 points along the inner arc of periphery $|\eta| \leq \eta_0$, which means that the lateral load in equation (1) is assumed by $q_k = Z_I/K$ with $K = 100$. The results that follow are for the series terms of equation (6) taken up to $M = 2$ and $N = 3$.

Figure 6 shows the variation of the blade tip displacement versus the depth of cut of the ingot x_I when the in-plane and the lateral forces acting on the blade is varied as shown in Figure 2. The displacement takes on the maximum at the maximum contact angle $\eta_0 = 39.42°$ or at the depth of cut $x_I/2a_I = 0.32$. It is also noted that the variation of the displacement is significant at the initial and finishing stages of slicing.

Figure 7 shows the variation of the blade deflection plotted with the operation speed Ω taken as a parameter. The in-plane and lateral forces applied at the edges were fixed at constant magnitudes. The displacement is nearly constant at the lower operation speeds, however it increases rapidly as the revolution speed approaches the first critical speed, i.e., the speed at which the frequency of (0,1) mode drops to zero.

Figure 8 is the variation of the blade deflection when the lateral force Z_I is increased. The displacement becomes greater monotonously with an increase of Z_I. Figure 9 shows the variation when the in-plane slicing load P is increased. It is noted from the figure that the in-plane force has no significant effect on the blade response. Finally, Figure 10 shows the variation of the displacement when the width of distribution of the lateral cutting force Z_I is varied, with the in-plane cutting force P retained at 3.14 N. The magnitude of lateral force acting per unit length of edge is $Z_I/(2\eta_I b\pi/180)$ N/m, where $2\eta_I°$ is the width of distribution of the lateral load. Comparison with Figure 8 shows that the tip deflection of the blade is much affected by the magnitude of the lateral load, but not to the width of the distribution.

CONCLUSIONS

(1) The initial tensioning has a significant effect on the natural frequencies of the working blade. The freqencies for the lateral vibration of the blade are much increased by the stresses from the tensioning. The stresses from the in-plane slicing load and the centrifugal force, on the other hand, have no noticeable effects on the blade frequencies.

(2) The lateral deflection of the blade is not much affected by the in-plane cutting force. On the other hand, it is sensitive to the variation of the lateral reaction force from the ingot. The lateral deflection becomes greater and takes on the maximum as the lateral force increases and comes to the maximum.

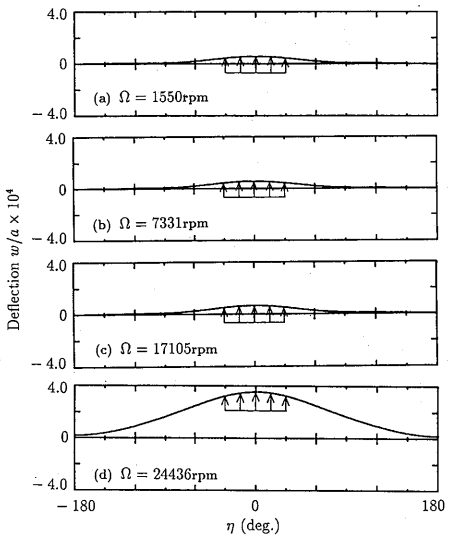

Fig. 7. Deflection of the blade inner edge with varied rotation speed Ω; $P = 290.74 \times 10^4$ N/m^2, $\theta_0 = 74.89°$, $Z_I = 3.14$ N, $\eta_0 = 30°$, $\sigma_0 = 7.05 \times 10^8$ N/m^2. (a) $\Omega = 1550$rpm; (b) $\Omega = 7331$rpm; (c) $\Omega = 17105$rpm; (d) $\Omega = 24436$rpm.

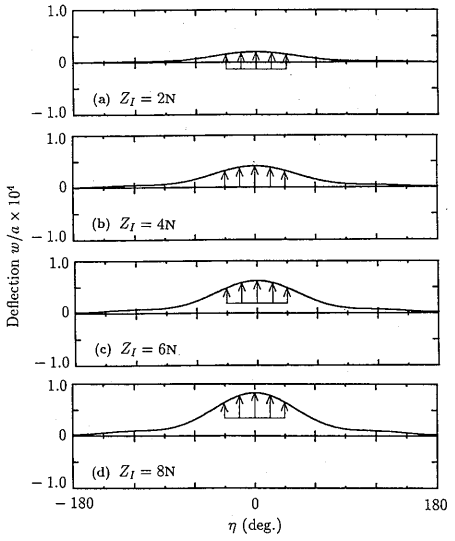

Fig. 8. Deflection of the blade inner edge with varied lateral load (Z_I); $\Omega = 1550$ rpm, $Z_I = 3.14$ N, $P = 290.74 \times 10^4$ N/m^2, $\theta_0 = 74.89°$, $\eta_0 = 30°$, $\sigma_0 = 7.05 \times 10^8$ N/m^2. (a) $Z_I = 2$N; (b) $Z_I = 4$N; (c) $Z_I = 6$N; (d) $Z_I = 8$N.

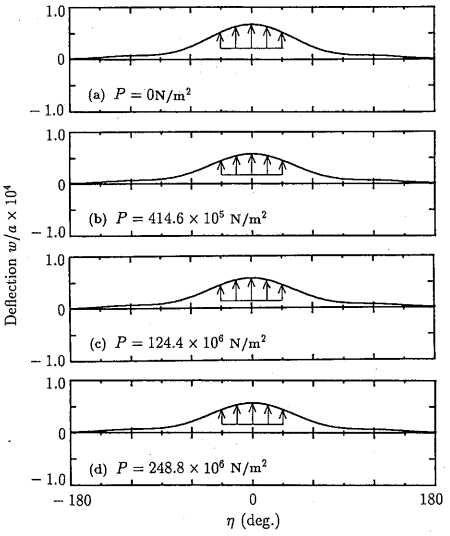

Fig. 9. Deflection of the blade inner edge with varied in-plane slicing load (P); $\Omega = 1550°$ rpm, $Z_I = 3.14$ N, $\theta_0 = 74.89°$, $\eta_0 = 30°$, $\sigma_0 = 7.05 \times 10^8$ N/m^2. (a) $P = 0$N/m^2; (b) $P = 414.6 \times 10^5$ N/m^2; (c) $P = 124.4 \times 10^6$ N/m^2; (d) $P = 248.8 \times 10^6$ N/m^2.

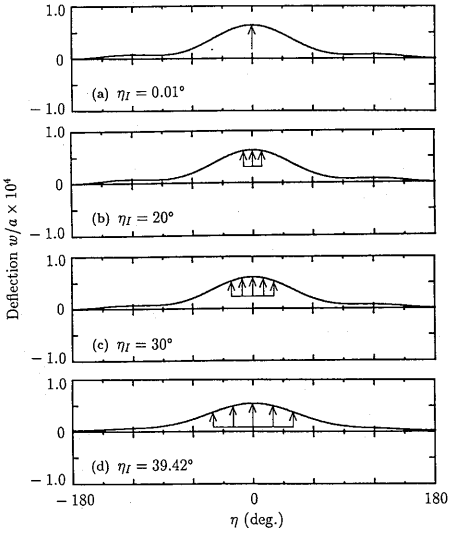

Fig. 10. Deflection of the blade inner edge with varied distribution of lateral load (η_I); $\Omega = 1550$ rpm, $Z_I = 3.14$ N, $P = 290.74 \times 10^4$ N/m^2, $\theta_0 = 74.89°$, $\eta_0 = 30.00°$, $\sigma_0 = 7.05 \times 10^8$ N/m^2. (a) $\eta_I = 0.01°$; (b) $\eta_I = 20°$; (c) $\eta_I = 30°$; (d) $\eta_I = 39.42°$.

REFERENCES

1. Iwan, W.D., and Moeller, T.L., ASME J. Appl. Mech., 43(1976), pp.485-490.
2. Radcliffe, C.J., and Mote, Jr. C.D., Inter. J. Mech. Sci., 19(1977), pp.567-574.
3. Srinivasan, V., and Ramamurti, V., Computers and Structures, 12(1980), pp.119-129.
4. Benson, R.C. and Bogy, D.B., ASME J. Appl. Mech., 45(1978), pp.636-642.
5. Ferguson, N.S., and White, R.G., J. Sound and Vib., 121(1988), pp.497-509.
6. Jiang, Z.W., Chonan, S., and Abé, H., ASME J. Vib. Acoust., 112(1990), pp.53-58.
7. Jiang, Z.W., and Chonan, S., Trans. JSME(C), 55-513(1989), pp.1157-1162.
8. Forman, S.E., and Rhines, W.J., J. Electrochemical Sciety, 119(1972), pp.686-690.
9. Chonan,S., and Sato,S., J. Sound and Vib., 127(1988), pp.245-252.
10. Chonan,S., Jiang,Z.W., and Yuki, Y., submitted for publication in ASME J. Vib. Acoust.